Antioxidant and UV-Blocking Properties of a Carboxymethyl Cellulose−Lignin Composite Film Produced from Oil Palm Empty Fruit Bunch

Muhammad T. Haqiqi, Wichanee Bankeeree, Pongtharin Lotrakul, Prasit Pattananuwat, Hunsa Punnapayak, Rico Ramadhan, Takaomi Kobayashi, Rudianto Amirta, and Sehanat Prasongsuk*

ACCESS | Metrics & More | Article Recommendations

ABSTRACT: Oil palm empty fruit bunch (EFB) pulp with the highest cellulose content of 83.42% was obtained from an optimized process of acid pretreatment (0.5% v/v H_2SO_4), alkaline extraction (15% w/w NaOH), and hydrogen peroxide bleaching (10% w/v H_2O_2), respectively. The EFB cellulose was carboxymethylated, and the obtained carboxymethyl cellulose (CMC) was readily water-soluble (81.32%). The EFB CMC was blended with glycerol and cast into a composite film. Lignin that precipitated from the EFB black liquor was also incorporated into the film at different concentrations, and its effect on the UV-blocking properties of the film was determined. Interestingly, the

EFB CMC film without lignin addition completely blocked UV-B transmittance. The incorporation of lignin at all concentrations significantly enhanced the UV-A blocking and other physical properties of the film, including the surface roughness, thickness, and thermal stability, although the tensile strength and water vapor permeability were not significantly affected. Complete UV-A and UV-B blocking were observed when lignin was added at 0.2% (w/v), and the film also exhibited the highest antioxidant activity against 2,2-diphenyl-1-picrylhydrazyl (DPPH) free radicals with an half-maximal inhibitory concentration (IC_{50}) value of 3.87 mg mL^{-1}.

INTRODUCTION

Environmental pollution caused by recalcitrant plastic wastes is increasingly contributing to severe ecological damage, both terrestrial and marine. Wildlife habitat and its biodiversity are harmed due to the contamination of plastic wastes, especially in the marine ecosystem.[1] Burning municipal solid waste (MSW) containing plastic in the open field also releases toxic gases, such as dioxins, furans, mercury, and polychlorinated biphenyl compounds.[2] Most plastic wastes take hundreds of years to degrade naturally under ambient conditions, and thus they accumulate in nature. Globally, over 150 million tonnes of plastic solid waste are produced every year.[3] Currently, the annual global plastic production is estimated to be about 300 million tonnes and is predicted to exceed 500 million tonnes by 2050.[4] Flexible plastic film is one of the most popular plastic products due to its superior properties, such as versatility, lightness, resistance, and printability.[5] The single-use and short-term application of the plastic film are believed to be one of the reasons for the increase in its waste accumulation in the environment. Since there is a massive demand for the plastic film, interest in developing a bio-based film substitute is growing due to the growing concerns on how to solve the negative environmental impacts from plastic waste.[6]

Biodegradable films offer the key advantage that they can be degraded by some living organisms. Lignocellulosic biomasses are one of the most promising sources for biodegradable film production due to their abundant availability, nontoxicity, and renewability. Cellulose is the largest composition in lignocellulosic biomass containing linear polymer chains of β-(1-4)-D-glucopyranose.[7] On the other hand, lignin has great potential for UV-blocking products due to its functional groups, such as phenol, ketones, and chromophores.[8] Besides UV-blocking, lignin also has another interesting property, namely, its antioxidant activity, which is due to its richness in phenolic hydroxyl groups.[9] Several attempts at lignocellulosic film development have been recently reported. Bian et al. reported that increasing lignin content in the lignocellulosic nanofibril (LCNF) film augmented its UV-blocking capacity and thermal stability.[10] Wei et al. demonstrated that

Table 1. Effect of Different Pretreatment Methods and Bleaching on the Yield and Composition of Cellulose Extracted from EFB by Alkaline Extraction[E]

	condition		pulp yield (g/100 g EFB)	cellulose content (%, w/w)	cellulose recovery (%, w/w)	hemicellulose content (%, w/w)	lignin content (%, w/w)
no	pretreatment	bleaching[D]					
1	untreated		62.03 ± 0.52^a	65.43 ± 0.33^e	94.37 ± 1.30^a	16.74 ± 0.95^a	12.42 ± 1.08^a
2	untreated	√	53.24 ± 0.27^c	67.45 ± 1.57^d	83.50 ± 0.89^d	14.96 ± 0.95^b	11.56 ± 0.68^{ab}
3	hot water[A]		56.89 ± 0.73^b	71.84 ± 0.84^c	95.04 ± 0.77^a	14.44 ± 0.87^b	8.84 ± 1.30^c
4	hot water[A]	√	51.21 ± 0.36^d	72.14 ± 0.88^c	85.90 ± 0.75^c	13.73 ± 0.41^b	8.63 ± 0.19^c
5	alkaline[B]		50.56 ± 0.46^d	74.98 ± 1.58^b	88.16 ± 0.90^b	10.48 ± 1.03^c	8.60 ± 0.90^c
6	alkaline[B]	√	44.78 ± 0.45^e	75.96 ± 0.83^b	79.09 ± 0.47^e	8.14 ± 0.60^d	7.85 ± 0.86^c
7	acid[C]		38.33 ± 0.86^f	82.26 ± 0.72^a	73.31 ± 1.39^f	2.17 ± 0.48^e	10.69 ± 0.57^b
8	acid[C]	√	35.01 ± 0.57^g	83.42 ± 0.88^a	67.92 ± 0.70^g	2.00 ± 0.43^e	8.79 ± 0.21^c

[A]Distilled water with a solid to liquid ratio of 1:6 at 121 °C for 40 min. [B]6% (w/v) sodium hydroxide with a solid to liquid ratio of 1:6 at 121 °C for 40 min. [C]0.5% (v/v) sulfuric acid with a solid to liquid ratio of 1:6 at 121 °C for 40 min. [D]10% (w/v) hydrogen peroxide with a solid to liquid ratio of 1:20 at 80 °C for 2 h. [E]Data were presented as the average value ± standard deviation. Different superscript letters in the same column indicated a significant difference at $p < 0.05$ in Duncan's multiple range test (DMRT) using IBM SPSS statistic 22 software.

incorporating lignin into the cellulose nanocrystal (CNC) film significantly enhanced its mechanical strength, UV-blocking properties, and antioxidant activity.[11] Furthermore, strong UV-light absorption, effective oxygen blockade, and good antibacterial performance were reported from the lignin-containing cationic wood nanofiber (CWNF) film.[12]

Although lignocellulosic films have reportedly shown several promising properties, a number of obstacles must be overcome, especially the certain characteristic of cellulose. Cellulose is not easy to melt and dissolve in water or in most common solvents due to its partially crystalline structure and strong inter- and intramolecular hydrogen bonds.[13] Consequently, cellulose-based films still have certain limitations, such as a brittle characteristic, poor mechanical behavior, and water sensitivity.[14] The conversion of cellulose into carboxymethyl cellulose (CMC) can evidently improve its film-forming properties as a hydrophilic polysaccharide. The attached carboxymethyl group disrupts the intra- and intermolecular hydrogen bonding between the cellulose chains and can form hydrogen bonds with water molecules.[15] The excellent tensile strength (TS), water vapor permeability (WVP), and thermal stability of CMC-based films were previously reported by several authors.[16−18] One of the most common methods to isolate lignin is alkaline extraction using sodium hydroxide (NaOH). This method can reportedly produce hydrophilic lignin with a lower molecular weight.[19] This water-soluble characteristic allows lignin to become compatible with CMC as a polymer matrix in composite film preparation. Furthermore, the interaction between the carboxymethyl groups of CMC and the phenolic hydroxyl groups of lignin opens up the opportunity for intermolecular hydrogen bonding formation.

Empty fruit bunch (EFB) is a solid agricultural waste produced in abundance annually from oil palm (*Elaeis guineensis*) crops, especially in Southeast Asian countries, including Indonesia, Malaysia, and Thailand. The oil palm industry produces approximately 1.1−1.5 tonnes of EFB per tonne of crude palm oil (CPO).[20] In practice, other oil palm residues, such as mesocarp fiber and palm kernel shell, are commonly utilized for boilers to generate electricity, but EFB is not suitable for these applications due to its high water content. Due to the lack of commercial opportunities, EFB is usually left at the plantation area for composting or EFB wastes are disposed of via open burning in some processing mills,

which contributes to hazardous air pollution that can affect human and animal health.[21] However, EFB wastes have recently attracted great attention due to their richness in cellulose (23.7−65.0%) and lignin (14.1−30.5%), which can potentially be extracted to increase their economic value.[22] However, a previous attempt to produce an EFB CMC product resulted in a film with low mechanical properties.[23] Hence, process development is required to increase the quality of the EFB CMC film. On the other hand, to the best of our knowledge, there is still no literature report on composite films produced from a combination of CMC and lignin prepared from EFB.

Herein, the production of a composite film using CMC and lignin prepared from EFB is reported. An efficient process to produce the EFB CMC was developed by first enhancing the cellulose purity by screening various chemical pretreatments, followed by alkaline extraction and hydrogen peroxide bleaching. The film characteristics obtained from the as-obtained EFB CMC samples were further assessed in comparison with commercial CMC and α-cellulose CMC films. Furthermore, the incorporation of EFB lignin into the EFB CMC film was also evaluated, especially regarding the improvement of the antioxidant property and UV-blocking performance. The results obtained from this study can form the basis for commercial process development for film production to valorize the abundant EFB waste.

■ RESULTS AND DISCUSSION

Screening for Efficient CMC Production. *Cellulose Extraction.* Based on the biomass composition analysis, the raw material (EFB) consisted of 43.17% cellulose, 23.24% hemicellulose, and 14.97% lignin. Without pretreatment, the NaOH extraction revealed a 0.5-fold increase of cellulose percentage (65.43%) in the EFB pulp; however, its residual hemicellulose (16.74%) and lignin (12.42%) contents were still high (Table 1). It has been previously reported that it is easier to cleave β-O-4 aryl ether bonds from lignin by NaOH treatment, whereas C−C bonds are relatively harder to break.[24] Hence, a high percentage of residual lignin was still found on the pulp. Also, the compact structure between the cellulose and hemicellulose in EFB could prevent the solvent from penetrating and degrading the hemicellulose.[25] Since cellulose is the most desirable material for converting into CMC, a strategy to enhance the effective separation between

the cellulose and other components was developed through incorporating a pretreatment and bleaching stage. The pretreated EFB samples had a significantly decreased pulp yield compared to unpretreated EFB (Table 1). The unpretreated EFB reached a yield of 62.03 g per 100 g of EFB, whereas EFB pretreated by hot water, alkaline, and acid solutions yielded 56.89, 50.56, and 38.33 g per 100 g EFB, respectively. Moreover, the H_2O_2 bleaching process showed a significant reduction (3−9%) in yield under each condition. The mass loss caused by the bleaching process indicated the further elimination of the EFB components, which was evidenced by the decrease in contents of hemicellulose and lignin (Table 1). As expected, the approach of applying various pretreatments to EFB had a significant impact on the cellulose content improvement compared to the unpretreated EFB, with yields of 71.84, 74.98, and 82.26% for the hot water, NaOH, and H_2SO_4 pretreatments, respectively. The significant enhancement of the cellulose content in EFB pulp achieved by H_2SO_4 pretreatment was similar to the previous study reported by Akhtar et al.[26] On the other hand, it was observed that the residual lignin was also reduced significantly, with values of 8.84, 8.60, and 10.69% for the hot water, NaOH, and H_2SO_4 pretreatments, respectively (Table 1). These results are in agreement with the previous study that reported that the highest reduction of β-O-4 lignin structures was reached following NaOH pretreatment, followed by hot water and H_2SO_4.[27]

Furthermore, chlorine-free bleaching using H_2O_2 of all EFB pulps showed a slight increase in the cellulose content. Among all of the tested conditions, H_2SO_4 pretreatment followed by NaOH extraction and H_2O_2 bleaching was revealed as the most efficient process by providing the highest cellulose content enhancement in EFB pulp (83.42%). Acid pretreatment using H_2SO_4 was reportedly able to break down the glycosidic linkage between hemicellulose and lignin effectively.[28] Therefore, the residual hemicellulose in the EFB pulp was reduced to the lowest level in this study (2.00%). It has been suggested that the better removal of hemicellulose is one of the key factors for the production of pulp containing high cellulose content.[29] This condition also provides some advantages since hemicellulose is an unwanted material for the composite film preparation. Although the low cellulose recovery indicated that the amount of cellulose was also degraded during the process, the optimized conditions in this study still revealed a higher cellulose content compared to the previous study (76.45%).[30]

CMC Production. The EFB pulps obtained under various conditions were further converted into CMC. Generally, the cellulose in the pulp was first modified with NaOH to form alkali cellulose, followed by the addition of sodium monochloroacetate (SMCA) to synthesize CMC. The yield and water solubility of the CMC products are shown in Table 2. It could be seen that unpretreated EFB with or without bleaching produced the highest yield (147.52−146.70 g per 100 g pulp). However, their water solubility was considerably low (45.51−48.63%). Similar results were observed for CMC products synthesized from both hot water- and NaOH-pretreated EFB pulp. These high yields were probably due to the presence of impurities, such as glycolic acid, sodium chloride, and sodium glycolate.[31] A high presence of sodium glycolate would enhance the toxicity of CMC, limiting its range of applications.[32] Furthermore, the hydroxyl groups on the residual lignin and hemicellulose might potentially be modified

Table 2. Effect of Different Pretreatment Methods and Bleaching to Obtain Extracted EFB Cellulose on the Yield and water Solubility of CMC Product[E]

no	condition		CMC yield (g/100 g EFB pulp)	water solubility (%, w/w)
	pretreatment	bleaching[D]		
1	untreated		147.52 ± 2.44[a]	45.51 ± 0.48[de]
2	untreated	√	146.70 ± 4.81[a]	48.63 ± 4.19[c-e]
3	hot water[A]		139.44 ± 1.01[b]	43.62 ± 4.57[de]
4	hot water[A]	√	146.53 ± 1.10[a]	54.65 ± 3.52[c]
5	alkaline[B]		127.31 ± 0.77[c]	42.37 ± 0.03[e]
6	alkaline[B]	√	127.32 ± 1.03[c]	49.69 ± 4.53[cd]
7	acid[C]		108.28 ± 0.96[e]	65.61 ± 2.04[b]
8	acid[C]	√	114.19 ± 1.95[d]	81.32 ± 1.53[a]

[A]Distilled water with a solid to liquid ratio of 1:6 at 121 °C for 40 min. [B]6% (w/v) sodium hydroxide with a solid to liquid ratio of 1:6 at 121 °C for 40 min. [C]0.5% (v/v) sulfuric acid with a solid to liquid ratio of 1:6 at 121 °C for 40 min. [D]10% (w/v) hydrogen peroxide with a solid to liquid ratio of 1:20 at 80 °C for 2 h. [E]Data were presented as the average value ± standard deviation. Different superscript letters in the same column indicated a significant difference at $p < 0.05$ in DMRT using IBM SPSS statistic 22 software.

during the etherification, thus affecting the increase in the yield attainable. Therefore, the optimized condition (EFB pulp derived from H_2SO_4 pretreatment, followed by NaOH extraction and H_2O_2 bleaching) achieved the most appropriate CMC product since it demonstrated the highest water solubility (81.32%). We concluded that a higher cellulose content could achieve higher efficiency in the carboxymethylation process.

The earlier study reported that the presence of lignin, even a small content, gave a lower efficiency in carboxymethyl cellulose synthesis.[33] In this study, the EFB cellulose used for CMC synthesis contained 8.79% residual lignin; thus, it might affect the process of carboxymethylation. Therefore, further measurement of the degree of substitution (DS) was performed. For comparison, the DS values of commercial CMC and α-cellulose CMC were evaluated. The DS value indicates the amount of −OH groups in the extracted cellulose substituted by carboxymethyl groups. Interestingly, EFB CMC achieved a higher average DS value (1.30) than that of commercial CMC (1.13), while α-cellulose CMC had an average DS value (1.45) higher than EFB CMC, probably due to its greater cellulose purity. More importantly, the obtained DS value of EFB CMC in this study was higher than the DS values of other CMC products prepared from rice stubble (0.64), seaweed (0.51), sugarcane bagasse (0.45−0.78), and cotton gin waste (0.87).[34−37] In line with the obtained DSs, the viscosity of α-cellulose CMC also had the highest value (41.81 mPa s), followed by EFB CMC and commercial CMC with the value of 19.92 and 18.54 mPa s, respectively.

Structural Analysis by Fourier Transform Infrared (FTIR). FTIR spectroscopy was performed to show the structural change behavior from the raw material up to the obtained EFB CMC product (Figure 1A). The prominent absorption observed at 3402 cm^{-1} in the FTIR spectra could be attributed to the stretching vibration of a hydroxyl group (−OH).[38] The peaks at 2921 and 2854 cm^{-1} of the raw material could be assigned to the bending of the aliphatic saturated C−H in cellulose, hemicellulose, and lignin.[30] The peak at 1728 cm^{-1} corresponded to the C=O nonconjugated vibration for hemicellulose.[39] Hence, the disappearance of this
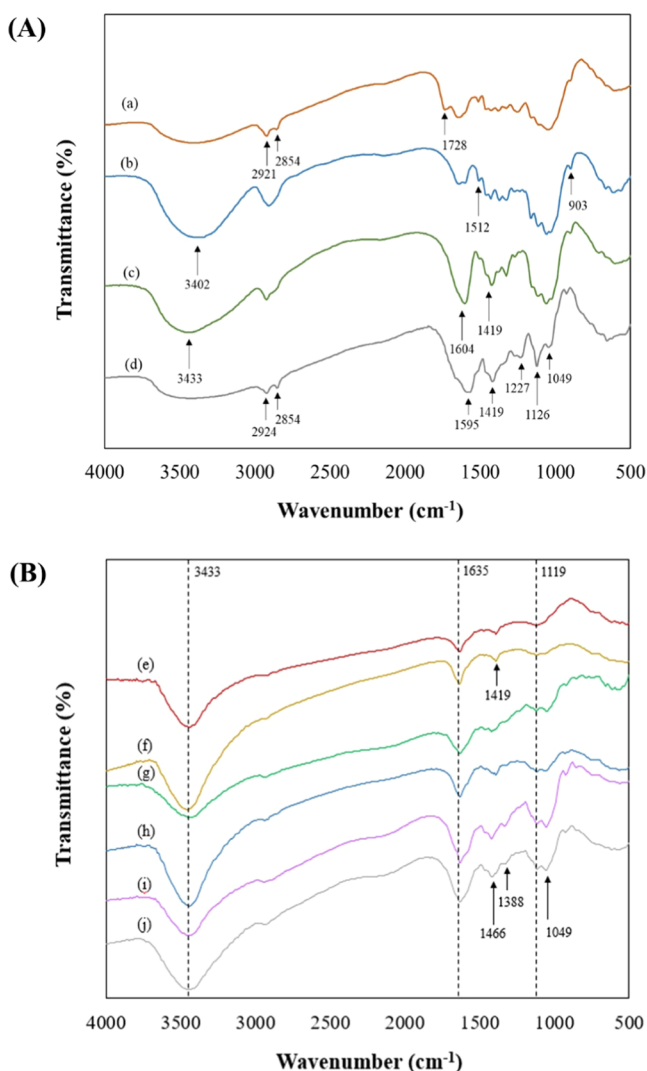
(A)

(B)

Figure 1. FTIR spectra of EFB (A): raw material (a), selected EFB cellulose extract (b), selected EFB CMC (c), and EFB lignin (d), and EFB CMC−lignin composite films (B): commercial CMC film (e), α-cellulose CMC film (f), EFB CMC film (g), EFB CMC + 0.1% EFB lignin film (h), EFB CMC + 0.2% EFB lignin film (i), and EFB CMC + 0.3% EFB lignin film (j).

peak indicated the successful degradation of the hemicellulose content. The presence of aromatic rings in lignin (C=C) in the extracted cellulose was detected from the peak at 1512 cm^{-1}.[40] The different structures of EFB pulp compared to commercial α-cellulose were detected at this wavenumber. The peak at 903 cm^{-1} represented the β-glycosidic bonds (C−O−C) in the anhydrous glucose units of cellulose.[41] Therefore, these results were consistent with the results from the biomass composition analysis. After carboxymethylation, the broad absorption peak at 3402 cm^{-1} was shifted to 3433 cm^{-1} due to the stretching frequency of −OH.[37] The structural changes observed at 1604 and 1419 cm^{-1} could be assigned to the C=O bond, which verified the successful carboxymethyl substitution in the EFB CMC sample.[42,43]

For EFB lignin, the peaks at 2924 and 2854 cm^{-1} in the spectra were ascribed to the C−H stretching vibrations from aliphatic groups (Figure 1A).[44] Aromatic skeletal vibrations appeared at 1595 and 1419 cm^{-1}, which indicated that the basic aromatic structure of lignin remained constant, even after

solubilization during the pretreatment process.[45] The peak at 1227 cm^{-1} confirmed the presence of phenolic −OH groups.[46] The peak at 1126 cm^{-1} corresponded to the vibration between C−H and C−O in the plane of the syringyl (S) units.[47] The characteristic C−O−C was observed at 1049 cm^{-1}, indicating the presence of carbohydrates as impurities.[46]

Film Characterization. *FTIR Spectra.* The FTIR spectra of the films ranging from 4000 to 500 cm^{-1} are shown in Figure 1B. A sharp absorption peak could be observed at 3433 cm^{-1}, presenting the hydrogen-bonded −OH.[48] The slight shift of the wavenumber from 1604 cm^{-1} to the higher band at 1635 cm^{-1} was related to the interaction of −COOH groups in all of the CMC films with −OH groups in glycerol. After incorporation of the EFB lignin, the peak at 1419 cm^{-1} in the EFB CMC film was slightly shifted to 1466 cm^{-1}, and a new peak appeared around 1388 cm^{-1}. The structural changes of the EFB CMC−lignin composite films observed according to the signals could be related to the interactions between EFB CMC and EFB lignin through intermolecular hydrogen bonding formation. The peaks detected at 1049 and 1119 cm^{-1} were due to −O− stretching.[16]

Surface Morphology. The scanning electron microscopy (SEM) images of the prepared films are shown in Figure 2A. The surfaces of the commercial CMC and α-cellulose CMC films were smooth and homogeneous due to the excellent interaction between each polymer matrix leading to the formation of a dense network. In contrast, the EFB CMC film had a rough surface, probably due to the residual lignin on the sample. However, there was no presence of micropores, bubbles, or cracks on the surface of all of the composite films. As the EFB lignin content increased, there were slight physical changes in the EFB CMC−lignin composite film surface roughness due to the presence of agglomerations. We stated that the EFB lignin particles (2.62−9.29 μm) were not well dispersed, indicating the low miscibility between the EFB lignin and EFB CMC. Some lignin particles formed hydrogen bonds among the lignin itself through the intermolecular interaction.[49] As reported by He et al., a similar situation was also found when lignin nanoparticles (LNPs) were loaded into poly(vinyl alcohol) (PVA).[9]

Color Properties. All of the composite films appeared to be transparent and homogeneous (Figure 2B). CMC typically produces a colorless film with excellent lightness, as can be seen for commercial CMC and α-cellulose CMC. In this study, the residual lignin contributed to producing a yellow color in the EFB CMC film. Thus, the addition of EFB lignin significantly changed the color parameters in the EFB CMC−lignin composite films, making them more reddish and yellowish, as proved by the increased *a* and *b* values, respectively (Table 3). Furthermore, the Δ*E* value increased with the increase in the EFB lignin concentration, demonstrating a significantly different color compared to a white standard. This phenomenon was due to the characteristic brown color of the EFB lignin. Therefore, the increasing EFB lignin content also affected the color of the EFB CMC−lignin composite films and made them become darker, resulting in a decrease in the lightness. However, the reduction in lightness is correlated with the positive ability of the EFB CMC−lignin films to offer UV-B (275−320 nm) and UV-A (320−380 nm) protection (Figure 4). Similar situations have also been reported in other lignin films.[50,51]

Thickness. The thickness is one of the essential parameters commonly affecting film performance, alongside water vapor or
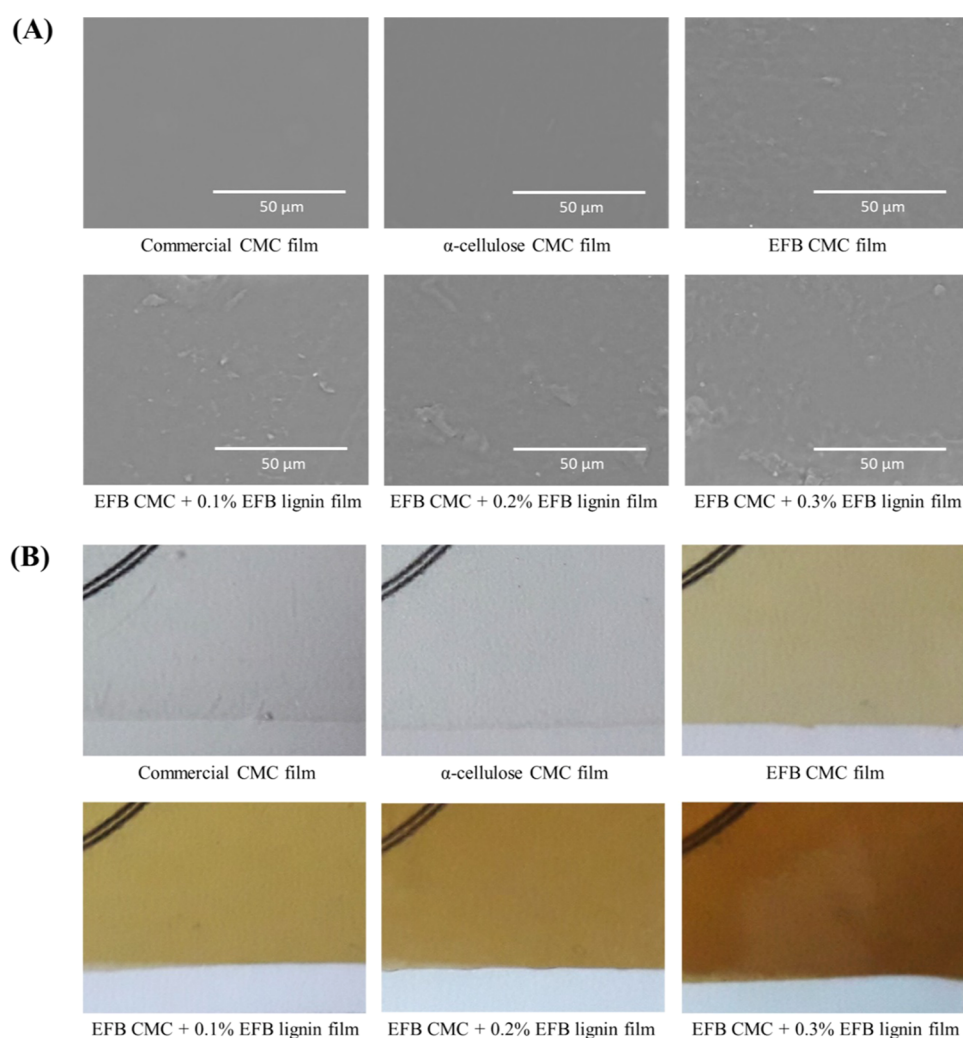
Figure 2. SEM (A) and photographic (B) images of all composite films.

Table 3. Color Properties of all Composite Films[a]

no	film	L	a	b	ΔE
1	commercial CMC	3.13	0.00	0.29	3.22
2	α-cellulose CMC	1.47	0.11	0.01	1.48
3	EFB CMC	6.68	1.36	14.69	8.71
4	EFB CMC + 0.1% EFB lignin	13.33	0.71	27.69	15.28
5	EFB CMC + 0.2% EFB lignin	19.68	4.05	37.24	21.87
6	EFB CMC + 0.3% EFB lignin	39.85	14.89	53.60	43.78

[a]L is the brightness/lightness; a indicates red (positive) or green (negative) color; b indicates yellow (positive) or blue (negative) color; and ΔE is the total color difference.

gas permeability and the mechanical properties.[52] In this work, the low standard deviation in the thickness measurements demonstrated the homogeneity of the cast film, as shown in Table 4. The mean thicknesses of commercial CMC, α-cellulose CMC, and EFB CMC films were 0.047, 0.060, and 0.054 mm, respectively. The value for the EFB CMC film thickness was in the middle position between the control films. When the smallest concentration of lignin (0.1%) was added into EFB CMC, there was no significant change in the thickness value. Then, with more lignin addition (0.2 and 0.3%), there was a significant increase in the film thickness to 0.057 and 0.061 mm, respectively. In line with these results,

Michelin et al. also reported that a commercial CMC-based film increased in thickness when organosolv lignin was added into it.[53]

Water Contact Angle. Contact angle measurement was used to determine the surface wettability of the prepared films. The results are summarized in Table 4. A film is characterized as hydrophobic when the contact angle value is more than 90°.[54] Since here, the values of the films were all lower than 90°, all of the composite films were considered to be hydrophilic. It was clearly observed that the EFB CMC film had a higher contact angle value (63.3°) than the α-cellulose CMC film (46.0°). This was related to the surface roughness of the film.[55] The addition of 0.1 and 0.2% EFB lignin into the EFB CMC film led to a significant decrease in the contact angle values to 56.0 and 53.3°, respectively. Furthermore, excessive EFB lignin loading (0.3%) dramatically reduced the value to 42.0°. In this study, EFB lignin was highly water-soluble, thus contributing to the increased hydrophilicity in the EFB CMC–lignin composite films. A similar result was reported by Zadeh et al., who revealed that the incorporation of lignosulfonates and hydrophilic alkali lignin into a soy protein isolate (SPI) film reduced the contact angle value.[56]

Water Vapor Permeability. The WVP represents the ability of a film to be a barrier material to reduce the transmission of water molecules through the film. Therefore, a lower WVP

Table 4. Thickness, Contact Angle, Water Vapor Permeability, and Thermal Properties of all Composite Films[B]

no	film	thickness (mm)	contact angle (deg)	WVP ($\times 10^{-11}$ g m^{-1} s^{-1} Pa^{-1})	T_{onset} (°C)	T_{max} (°C)	weight loss (%)	char residue (%)
1	commercial CMC	0.047 ± 0.00^d	ND[A]	6.66 ± 0.49^b	158.9	271.2	72.91	27.09
2	α-cellulose CMC	0.060 ± 0.00^{ab}	46.0 ± 1.7^c	7.55 ± 0.13^a	152.8	275.9	73.63	26.37
3	EFB CMC	0.054 ± 0.01^c	63.3 ± 1.2^a	7.24 ± 0.39^{ab}	124.5	272.6	73.08	26.92
4	EFB CMC + 0.1% EFB lignin	0.054 ± 0.01^c	56.0 ± 2.0^b	7.56 ± 0.39^a	145.7	269.8	71.69	28.31
5	EFB CMC + 0.2% EFB lignin	0.057 ± 0.01^{ab}	53.3 ± 2.3^b	7.68 ± 0.44^a	145.9	269.6	71.48	28.52
6	EFB CMC + 0.3% EFB lignin	0.061 ± 0.00^a	42.0 ± 1.0^d	7.76 ± 0.30^a	146.6	266.2	70.27	29.73

[A]Not detectable, the commercial CMC film was very sensitive when touching the water on its surface. [B]T_{onset} is the temperature that contributes to the beginning decomposition of the film; T_{max} is the temperature that contributes to the maximum weight loss rate of the film based on the derivative thermogravimetry (DTG) curve. Different superscript letters in the same column indicated a significant difference at $p < 0.05$ in DMRT using IBM SPSS statistic 22 software.
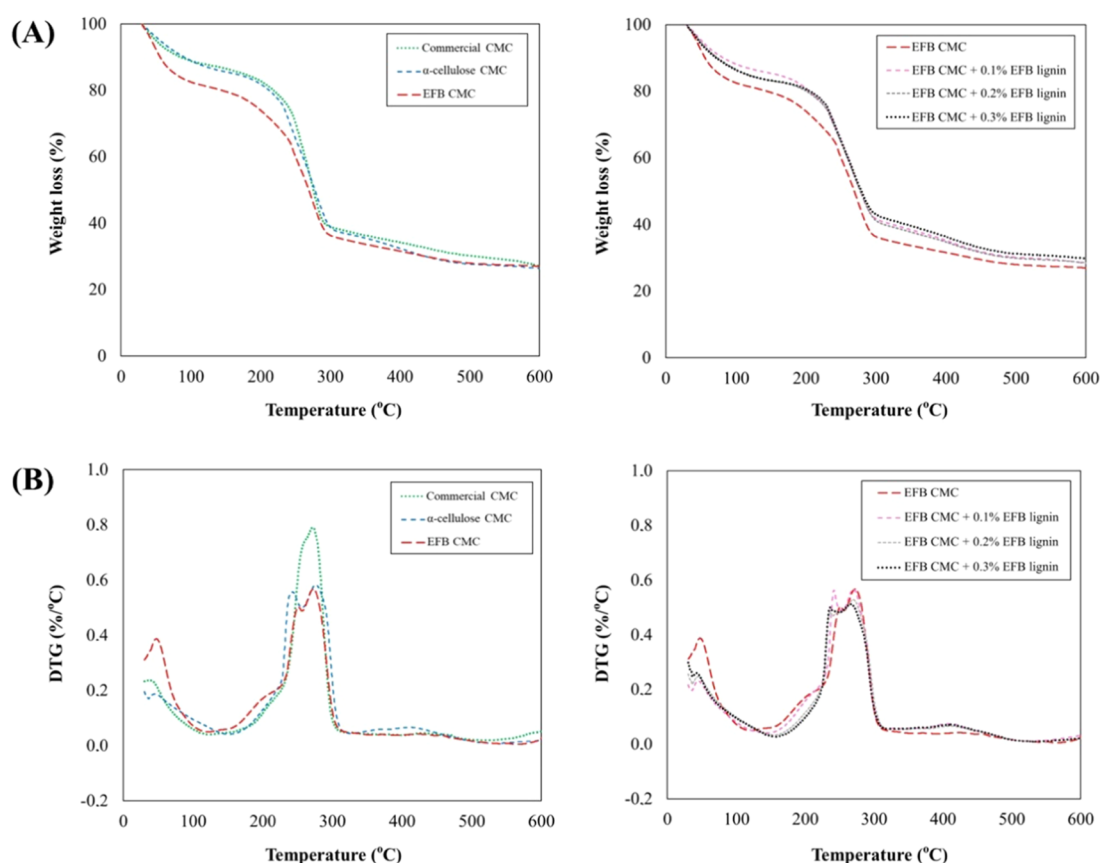

Figure 3. TGA (A) and DTG (B) curves of all composite films.

indicates a better barrier property toward water vapor. In this study, the commercial CMC film achieved the lowest WVP (6.66×10^{-11} g m^{-1} s^{-1} Pa^{-1}) (Table 4). This WVP value of the commercial CMC film was not significantly different from that of the EFB CMC film (7.24×10^{-11} g m^{-1} s^{-1} Pa^{-1}). On the other hand, the WVP of the α-cellulose CMC film was relatively high (7.55×10^{-11} g m^{-1} s^{-1} Pa^{-1}), indicating its low performance compared to the commercial CMC film. Although there was no significant change in WVP after the addition of EFB lignin in all concentrations, a slight acceleration in water vapor diffusion was observed with the increase in lignin loading. These results were strongly related to the hydrophilic character of EFB lignin, whereby the free hydroxyl groups in the composite films could easily interact

with water vapor molecules. In addition, the absorbance of water molecules by the film matrix also depends on the environmental conditions, whereby an increase in temperature and relative humidity will increase the water vapor permeability of the film.[57]

Thermal Properties. The thermal stability of the prepared films was determined by thermogravimetric analysis (TGA). The heating process in TGA decomposes bonds within the molecules of a material.[18] The TGA and derivative thermogravimetry (DTG) curves are displayed in Figure 3. In general, all of the prepared films decomposed in three main stages. The first stage, which occurred between 50 and 150 °C, was related to water molecule evaporation. The second stage was mainly associated with glycerol volatilization and

Table 5. DPPH Radical Scavenging Activity (RSA) and IC$_{50}$ Value of all Composite Films[B]

no	film	radical scavenging activity (%)					IC$_{50}$ (mg mL^{-1})
		0.25 mg mL^{-1}	0.5 mg mL^{-1}	1 mg mL^{-1}	2 mg mL^{-1}	4 mg mL^{-1}	
1	commercial CMC	ND[A]	ND[A]	ND[A]	ND[A]	ND[A]	ND[A]
2	α-cellulose CMC	ND[A]	ND[A]	ND[A]	ND[A]	ND[A]	ND[A]
3	EFB CMC	3.23 ± 0.26[c]	3.90 ± 0.33[d]	7.29 ± 2.22[c]	11.85 ± 1.82[c]	20.41 ± 0.42[d]	10.34 ± 0.22[a]
4	EFB CMC + 0.1% EFB lignin	3.24 ± 0.09[c]	7.42 ± 1.12[c]	13.60 ± 1.06[b]	20.57 ± 2.13[b]	33.64 ± 2.86[c]	6.01 ± 0.60[b]
5	EFB CMC + 0.2% EFB lignin	6.53 ± 0.47[b]	13.68 ± 0.66[b]	22.83 ± 1.17[a]	34.57 ± 0.86[a]	48.63 ± 1.80[b]	3.87 ± 0.16[c]
6	EFB CMC + 0.3% EFB lignin	7.78 ± 0.49[a]	15.25 ± 0.77[a]	25.16 ± 2.15[a]	35.34 ± 0.22[a]	52.11 ± 0.19[a]	3.27 ± 0.09[c]

[A]Not detectable, no inhibition was found. [B]Data were presented as the average value ± standard deviation. Different superscript letters in the same column indicated a significant difference at $p < 0.05$ in DMRT using IBM SPSS statistic 22 software.

saccharide ring dehydration in CMC, where the different reaction mechanisms observed from the presence of the second peak were attributed to dehydroxylation and the pyrolytic fragmentation process in CMC.[58−60] The maximum value of weight loss occurred in this stage, which can be seen from the T_{max} in the DTG curves. It could be observed that the T_{max} value of the EFB CMC film was higher than those of all EFB CMC−lignin composite films (Table 4). This phenomenon was probably due to the thermal decomposition of α- and β-aryl-alkyl-ether bonds in lignin, which commonly occurred at lower temperatures (150−300 °C), contributing to the reduction in their T_{max}.[61] The last stage, which occurred above 400 °C, was related to oxidation and the breakdown of the carbonaceous material residue.[62]

The EFB CMC film achieved a low T_{onset}, indicating poor thermal stability (Table 4). After EFB lignin incorporation, T_{onset} was drastically improved as the EFB lignin concentration increased. This demonstrated that the introduction of EFB lignin made a positive contribution to the thermal stability. The interaction of EFB lignin with EFB CMC in this work was in line with the literature stating that lignin can act as a thermal stabilizer due to its richness in phenolic hydroxyl groups.[63] In this study, EFB lignin also raised the percentage of char residue and decreased the total weight loss of the EFB CMC−lignin composite films at the end of the process.

Antioxidant Activity. Since free radicals are harmful to both biotic and abiotic entities, it is of interest to access the ability to scavenge radicals (antioxidant capacity) of the film.[64] The decolorization of 2,2-diphenyl-1-picrylhydrazyl (DPPH) after reacting with the film solution was observed and noted as an indicator of the antioxidant activity. The DPPH radical scavenging activity (RSA) and half-maximal inhibitory concentration (IC$_{50}$) values are presented in Table 5. It could be seen that the commercial CMC and α-cellulose CMC films did not show any inhibition of the DPPH radicals. These results were similar to a previous study, which reported that a common commercial CMC film exhibited negligible radical scavenging activity.[53] Interestingly, the EFB CMC film was active against DPHH-free radicals (IC$_{50}$, 10.34 mg mL^{-1}). The residual lignin on the EFB CMC films could be the reason for the significant difference with the commercial CMC films through its contribution as a radical scavenger. As reported, lignin has antioxidant activity through the available phenolic hydroxyl groups, which can react with free radicals by delivering one electron and one proton.[65] Hence, the RSA was significantly improved with the increased concentration of EFB lignin in the EFB CMC−lignin composite film. The IC$_{50}$ values of the EFB CMC film after 0.1, 0.2, and 0.3% EFB lignin incorporation were 6.01, 3.27, and 3.87 mg mL^{-1}, respectively. The IC$_{50}$ value gradually decreased with the increase in the

EFB lignin content, illustrating that the antioxidant activity became higher. Among these concentrations, an insignificant difference between 0.2 and 0.3% EFB lignin addition was found, indicating that a further higher EFB lignin incorporation had a limited effect on the enhancement of the antioxidant activity.

Several authors have studied the improvement of the antioxidant activity in films by lignin addition. For instance, Avelino et al. evaluated the effect of the incorporation of various lignin soluble factions at 1 wt % on the poly(methyl methacrylate) (PMMA) film and reported IC$_{50}$ values of 40, 27, and 28 mg mL^{-1} for a PMMA−WCSAL film, PMMA−ACT-F film, and PMMA−EtOH film, respectively.[63] Aadil et al. reported that a gelatin−lignin film achieved its highest radical scavenging activity (67%) after incorporating 40% (w/v) lignin (IC$_{50}$ = 111.10 μg mL^{-1}).[66] A similar work involving the commercial CMC−lignin film was previously reported by Michelin et al., who found that the CMC−lignin film achieved an IC$_{50}$ value of 50 μg$_{lignin}$ mL^{-1}.[53] In this study, the optimized composition of the EFB CMC−lignin composite film had an IC$_{50}$ value of 3.27 mg mL^{-1}, which was equivalent to the addition of EFB lignin at 65 μg$_{lignin}$ mL^{-1}. This finding confirmed that the EFB lignin exhibited a slightly lower antioxidant activity. The presence of carbohydrates as impurities in the EFB lignin might have affected the lignin and led to a decrease in its antioxidant properties since the polar groups of the carbohydrate impurities could have formed hydrogen bonds with the phenolic groups of the lignin.[67] This was similar to the previous report by Pei et al. that a higher percentage of carbohydrates in the lignin complex could result in antioxidant potency reduction.[68] According to Guo et al., a high content of phenolic hydroxyl groups in lignin could enhance the antiradical activity.[69] Meanwhile, the aliphatic hydroxyl groups have a converse effect.[19] Nevertheless, it could be said that the EFB CMC−lignin composite film has potential application for active packaging due to its antioxidant activity.

UV-Blocking Capacity. The transmittance of the prepared films was recorded in the wavelength ranging from 200 to 800 nm using a UV−vis spectrophotometer (Figure 4). The results showed that the EFB CMC film exhibited a high UV-blocking capacity, reaching 100% UV-B blocking, while the commercial CMC and α-cellulose CMC films did not possess this ability. Again, in this study, we believe that the residual lignin on the EFB CMC film had a strong impact on its ability to absorb UV-light as the further addition of EFB lignin into the EFB CMC film led to improving the UV-blocking ability, especially in the UV-A region. As shown in Figure 4, the incorporation of 0.2 and 0.3% EFB lignin additions could block 100% of the UV-A. Meanwhile, the incorporation of EFB lignin also led to reducing the transparency of the EFB CMC−lignin composite
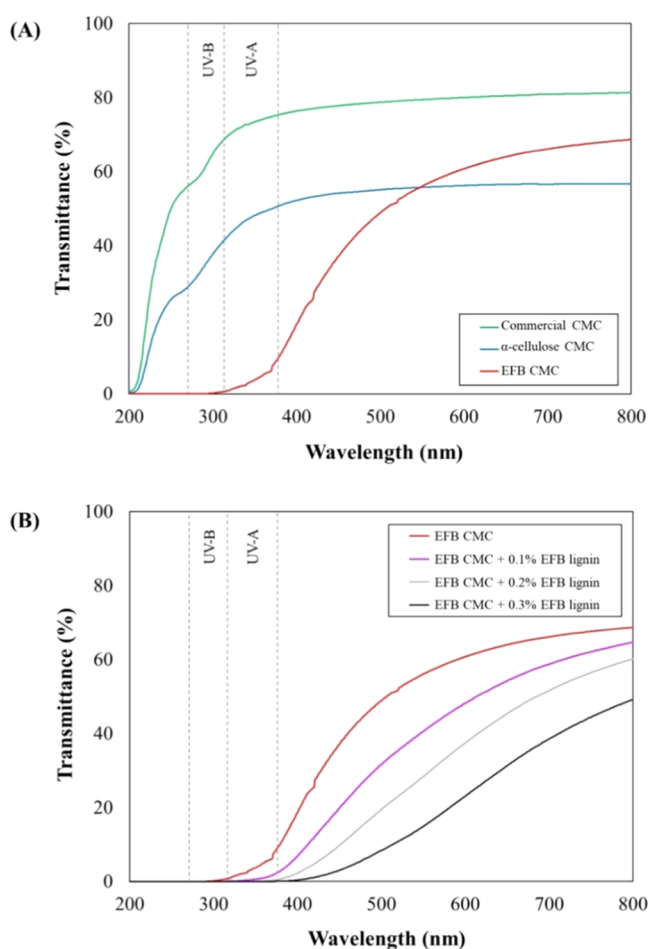
Figure 4. Transmittance profile of CMC-based films (A) and EFB CMC–lignin composite films (B).

film. It could be seen that 0.3% EFB lignin addition led to a decrease in transparency compared to 0.2% EFB lignin addition. Therefore, EFB CMC–lignin with a concentration of 0.2% EFB lignin was found to be the best proportion to block UV-light effectively. These results were consistent with the previous report that reported that the addition of lignin will increase the UV protection and decrease the transparency of the cellulose-based film.[70] Abundant lignin chromophores, including hydrophilic phenolic hydroxyl groups, have been reported to be able to block the UV light by absorbing its photon energy and further converting it to heat.[65]

Izaguirre et al. incorporated different lignin solutions dissolved in ethyl acetate, ethanol, methanol, and acetone into chitosan films and found that the UV transmittance from the obtained films dropped considerably, even though the UV-A and UV-B regions were not totally blocked at the lignin concentrations used.[51] Sadeghifar et al. developed a commercial cellulose film containing 2 wt % lignin that demonstrated total UV-B and more than 90% UV-A blocking.[70] Similarly, effective UV-B blocking was found when lignin was added at a higher concentration (3 wt %) into the PVA film, whereas UV-A transmittance was still not totally barred.[71] Furthermore, Parit et al. reported that complete UV-A and UV-B blocking was obtained in the cellulose nanocrystal (CNC)/lignin film at a 10 wt % softwood kraft lignin loading.[72] A lower lignin addition to bar all UV transmittance was reported by Zhang et al. when applying 5 wt

%, equal to 0.25% (w/v), lignin nanomicelle (LNM) incorporation into a PVA/LNM composite film.[73] This result was comparable with our study, which showed that even the addition of 0.2% (w/v) EFB lignin into the EFB CMC–lignin composite film could block both UV-A and UV-B completely. Therefore, the high UV-absorption ability of the EFB CMC–lignin composite film indicates that the film could potentially be used as a UV-blocking packaging product.

Mechanical Properties. Films are commonly designed to resist stress during handling, storage, and shipping.[74] Therefore, the mechanical performances of the prepared films were evaluated using a universal testing machine (Figure 5). There were no statistically significant differences between the commercial CMC, α-cellulose CMC, and EFB CMC films in terms of their tensile strength (TS), with values of 30.27, 31.56, and 33.87 MPa, respectively. A previous study reported that a CMC-based film prepared from EFB resulted in a relatively low TS compared to commercial CMC.[23] Interestingly, in this study, we achieved a better value (33.87 MPa), indicating our superior EFB CMC film preparation. Since our EFB CMC–lignin composite films achieved greater tensile strength values, these results suggest that the film would be competitive with some conventional polyester packaging films that are commercially available on the market, such as low-density polyethylene (8−10 MPa), high-density polyethylene (19−31 MPa), ethylene vinyl alcohol (6−19 MPa), poly-caprolactone (4 MPa), polystyrene (31−49 MPa), and polypropylene (27−98 MPa).[75]

The most significant difference among EFB CMC, commercial CMC, and α-cellulose CMC films was found in the measurement of the elongation at break (EB), where it was observed that α-cellulose CMC had the highest EB (24.47%), followed by EFB CMC (13.79%) and commercial CMC (8.33%). This pattern seems to suggest that these results were related to the obtained DS value of each CMC sample. The high carboxymethyl substituent provides more intermolecular interactions between polymer chains.[16] When EFB lignin was incorporated into the EFB CMC film, the EB value dropped drastically, especially when adding the highest EFB lignin concentration (0.3%). This was also confirmed by the presence of some agglomerations in the EFB CMC–lignin composite film surface. Agglomerations can lead to a premature rupturing of the materials and contribute to a decline in the film elasticity.[76] On the other hand, a significant increase in the Young's modulus (YM) was also detected after the addition of the maximum EFB lignin concentration (0.3%). Such an increase in the YM value was contributed by the slight enhance in mechanical strength and the significant decrease in film elongation. A higher value of YM is not desirable since it corresponds to the stiffness of a film.[77] These findings suggest that the much higher lignin incorporation led to an increased roughness and brittleness in the EFB CMC–lignin composite film, which is unfavorable for the desired mechanical performance.

■ CONCLUSIONS

In summary, the most efficient EFB CMC production was achieved from the conversion of extracted EFB pulp prepared by H_2SO_4 pretreatment followed by NaOH extraction and a H_2O_2 bleaching stage. Interestingly, significant differences between commercial CMC, α-cellulose CMC, and EFB CMC films were found, whereby the EFB CMC film had a high antioxidant activity and total UV-B blocking capacity. Although
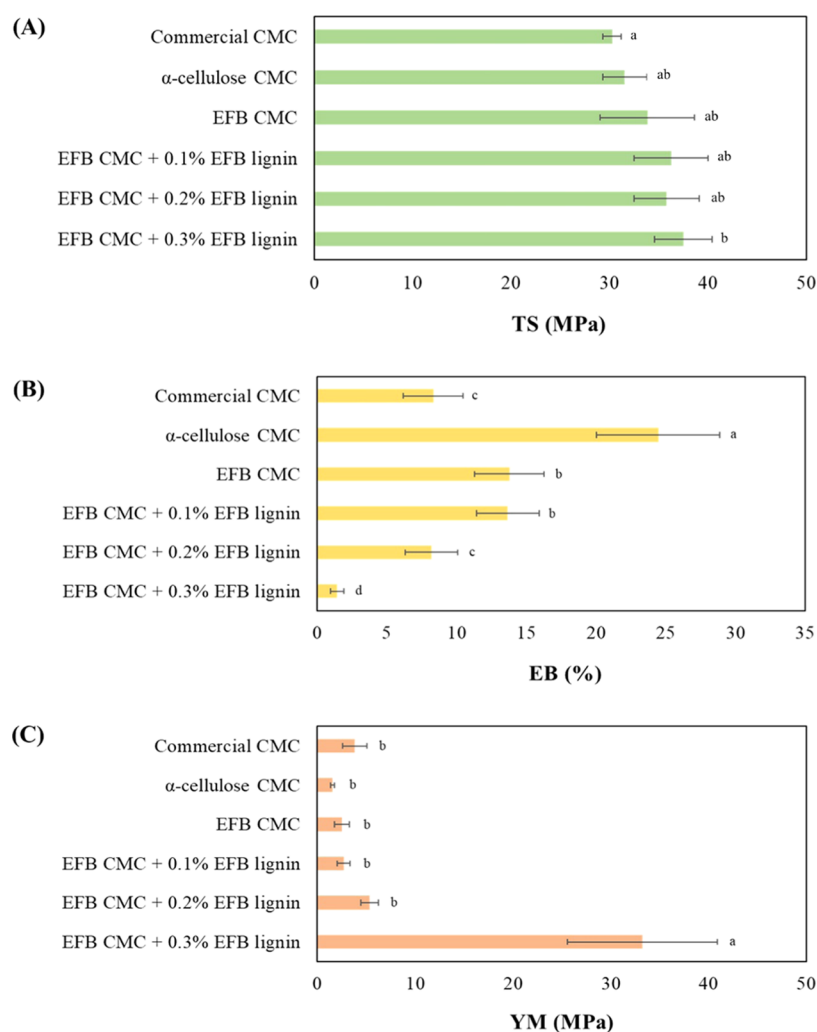
Figure 5. Mechanical properties of all composite films: tensile strength (A), elongation at break (EB) (B), and Young's modulus (YM) (C). Different letters in the same graph indicated a significant difference at $p < 0.05$.

it had a rough surface, dark color, and lower thermal stabilities, other properties, such as its thickness, surface hydrophilicity, mechanical properties, and water vapor permeability, were comparable with those films prepared from commercial compounds. EFB CMC supplemented with 0.2% EFB lignin was found to be the optimized composition among all of the tested EFB lignin concentrations according to its highest antioxidant activity, total UV-A and UV-B blocking capacity, and preferable mechanical performance. The lignin-containing CMC film demonstrated a great potential for future development to produce antioxidant and UV-blocking materials from the otherwise unprofitable EFB.

■ EXPERIMENTAL SECTION

Materials. EFB was provided by PT. Tritunggal Sentra Buana (TSB, PT), an oil palm mill located at Muara Badak District, Kutai Kartanegara, East Kalimantan, Indonesia. The EFB was hard cut, grounded, and sieved to small pieces (≤1 mm), followed by drying in a hot oven until a constant weight was reached.

Cellulose Extraction. *Screening for Suitable Pretreatment.* To screen for an efficient pretreatment, three methods using hot water, alkaline (6% NaOH, w/v), and acid (0.5% H_2SO_4, v/v) were performed with a solid/liquid ratio of 1:6 in

an autoclave (121 °C, 15 lbs in.$^{-2}$ for 40 min).[78] After pretreatment, the EFB pulp was left to cool down to room temperature. The EFB pulp was then filtrated, washed several times with distilled water, and dried in a hot air oven at 60 °C until a constant weight was reached.

Extraction. Alkaline extraction was employed to isolate cellulose from each pretreated EFB pulp using 15% (w/w) NaOH at a solid/liquid ratio of 1:10. The process was carried out in an autoclave (121 °C, 15 lbs in.$^{-2}$) for 1 h. The obtained pulp was separated from black liquor by filtration through a plastic sieve. The black liquor was kept for subsequent lignin isolation in an opaque bottle at room temperature. The pulp was then neutralized with a large volume of distilled water and oven-dried at 60 °C.

Bleaching. Totally chlorine-free bleaching was conducted according to the protocol introduced by Tristantini and Yunan.[79] A liquid solution containing 10% (w/v) of H_2O_2 was prepared to bleach the EFB pulp in a solid/liquid ratio of 1:20. The experiment was performed by heating at 80 °C for 2 h under continuous stirring conditions. The bleached pulp was filtered, washed repeatedly with distilled water until neutrality, and dried at 60 °C.

Lignin Precipitation. Lignin was recovered from the black liquor by acid precipitation. Precipitation was performed by

adding glacial acetic acid to the black liquor until pH was 7. Lignin pellet was collected by centrifugation at 12 000g for 10 min, followed by drying at 60 °C. The particle size of the EFB lignin was measured using a laser-based Malvern Mastersizer 2000 (Malvern Instrument Ltd., U.K.).

Carboxymethyl Cellulose Synthesis. CMC was synthesized from EFB cellulose according to Asl et al. with slight modifications.[36] Briefly, the EFB pulp (5 g) was stirred in 20 mL of 30% (w/v) NaOH and 200 ml of isopropanol at room temperature for 30 min. Five grams of sodium monochloroacetate (SMCA) was then added to the mixture and stirred at 60 °C for 4 h. Then, the liquid was removed, and the solid precipitate was suspended in 150 mL of absolute methanol. The solution was then neutralized by glacial acetic acid, filtered, and washed with 70% ethanol to remove unwanted salt. The solid CMC was washed again with absolute methanol. Finally, the CMC product was obtained after oven drying at 60 °C until it reached a constant weight. A commercial α-cellulose (C8002, Sigma-Aldrich) was also used for CMC synthesis following the same procedure. The viscosity of the synthesized CMC (2.5% w/v) was measured at ambient conditions with a shear rate of 100 s^{-1} using a rheometer (Physica MCR 301, Anton Paar, Germany).

Composite Film Production. Composite films were prepared using a solution casting method. EFB CMC powder was dissolved in distilled water at 60 °C with continuous stirring to prepare a 2.5% (w/v) CMC solution. Glycerol as a plasticizer was added to the CMC solution to a final concentration of 0.5% (v/v). The lignin solution was prepared by dissolving the EFB lignin powder in distilled water at 80 °C for 1 h under stirring conditions. The lignin solution was then added to the CMC−glycerol mixtures at different final concentrations ranging from 0 to 0.3% (w/v). The mixtures were stirred continuously for another hour to obtain homogenous solutions. Each obtained film-forming solution (20 mL) was poured into a film mold (5 × 15 cm^2) and dried in a hot air oven at 60 °C for 24 h. The dried films were carefully peeled off from the mold and were conditioned inside a desiccator containing silica gel at least 24 h before further assessments. The films prepared from commercial CMC (C5678, Sigma-Aldrich) and α-cellulose CMC were also prepared for property comparison.

Biomass, CMC, and Film Characterization. *Determination of Biomass Composition.* Biomass compositions, including cellulose, hemicellulose, and lignin of EFB and the obtained pulp, were determined according to Goering and Van Soest.[80]

Water Solubility. The water solubility of the EFB CMC powder was performed according to Shui et al. with a slight modification.[31] The EFB CMC powder (0.5 g) was dissolved in 50 mL of distilled water at 60 °C for 1 h under continuous stirring conditions. The remaining solid residue was then collected by centrifugation at 10 000g for 10 min, oven-dried at 60 °C, and weighed. The percent solubility was calculated as the percentage of dissolved EFB CMC to total EFB CMC tested.

Degree of Substitution. The degree of substitution (DS) of the CMC was examined by potentiometric titration.[37] One gram of the CMC was mixed with 50 mL of 95% ethanol under stirring conditions at room temperature. Five milliliter of 2 M nitric acid was then dropped into the mixture with continuous stirring for 10 min. After that, the mixture was boiled for 5 min followed by further stirring for 20 min. The solid CMC was

filtered through filter paper (Whatman no. 1) and washed with 100 mL of 95% ethanol, followed by oven drying at 60 °C. The obtained CMC (0.5 g) was then dissolved in 100 mL of distilled water before 25 mL of 0.5 M NaOH was added to the solution. The mixture was boiled for 20 min and cooled down to room temperature before a few drops of phenolphthalein as an indicator was added. The mixture was then titrated with 0.3 M HCl until the color was changed. The DS was calculated using the following equation

$$A = \frac{(BC - DE)}{F} \tag{1}$$

$$DS = \frac{(0.162 \times A)}{(1 - 0.0058 \times A)} \tag{2}$$

where A was the milliequivalents of required acid used per gram of CMC, B was the volume of required NaOH, C was the concentration of NaOH, D was the volume of required HCl, E was the concentration of HCl, F was the weight of CMC (g), 162 was the molecular weight of anhydrous glucose, and 58 was the net molecular weight increase in anhydrous glucose after each carboxymethyl group substitution.

Fourier Transform Infrared (FTIR) Spectroscopy. Infrared spectra of the samples were recorded using a Fourier transform infrared (FTIR) spectrometer (Nicolet 6700, Thermo Nicolet Corp, Madison) in the wavenumbers between 4000 and 400 cm^{-1}. Potassium bromide (KBr) was mixed with the sample at a ratio of 10:1 (by weight) and pelletized together before testing.

Scanning Electron Microscopy. The surface morphology of the films was observed using a scanning electron microscope (SEM) (TM3030 Plus, Hitachi, Japan). First, the film samples were gold-coated using a quick cold coater (SC-701MC, Sanyu Denshi Co., Ltd., Japan). Images were taken at an accelerating voltage of 15 kV and at magnifications of 1500×.

Color Measurement. The color of the film samples was determined using a spectrophotometer (Color-eye 7000, Macbeth, New Windsor, NY). The parameter of lightness− brightness (L), redness−greenness (a), and yellowness− blueness (b) were recorded. The total color difference (ΔE) was calculated according to the following equation[81]

$$\Delta E = \sqrt{(L^* - L)^2 + (a^* - a)^2 + (b^* - b)^2} \tag{3}$$

where L^*, a^*, and b^* were the value of the standard, and L, a, and b were the values measured from the film samples.

Thickness. The average thickness of the prepared films was measured randomly at 10 different areas using a micrometer screw gauge (Mitutoyo, Japan) with a minimum division value of 0.01 mm.

Water Contact Angle. The water contact angle was measured by a sessile drop method using a contact angle goniometer (DM100, Kyowa Interface Science Co., Ltd., Japan). Square films with a size of 2 × 2 cm^2 were prepared, and a microsyringe injected a drop of distilled water on the horizontal surface of the films.

Water Vapor Permeability. The water vapor permeability (WVP) was determined gravimetrically using a cup method according to the standard of ASTM E 96. The film was cut in a circular shape and sealed with silicone on the top of the cup (5 cm in diameter and 4 cm depth) containing 15 mL of distilled water. Then, the WVP cup was placed in a box containing silica gel. The tests were carried out at 30 °C by measuring the water

weight every hour for at least 8 h to obtain the slope of the linear regression of weight loss versus time ($r^2 = 0.99$). The WVP ($g\ m^{-1}\ s^{-1}\ Pa^{-1}$) was calculated based on the following equation[82]

$$\text{WVP} = \frac{\Delta w \times x}{\Delta t \times A \times \Delta P} \qquad (4)$$

where Δw was the measured weight loss of WVP cup (g), x was the thickness of the film (m), Δt was the unit of time (s), A was the exposed area (m^2), and ΔP (4245 Pa) was the difference in partial water vapor pressure across the two sides of the film.

Thermogravimetric Analysis. The thermal analysis of prepared films was performed by a thermogravimetric analyzer (TGA Q50, TA Instruments, Inc., DE). A quantity of 5 mg of each sample was tested under a nitrogen atmosphere at a flow rate of 20 mL min^{-1}. The sample was heated from 30 to 600 °C at a rate of 10 °C min^{-1}.

Antioxidant Activities. The antioxidant activity of the films was evaluated using the 2,2-diphenyl-1-picrylhydrazyl (DPPH) free radical scavenging assay according to Shankar et al. with slight modifications.[83] First, the film was solubilized in distilled water. The aqueous solution of the film (100 μL) was then added to 900 μL of 0.1 mM DPPH methanolic solution. The solution was incubated for 30 min in the dark at room temperature. The antioxidant activity was measured at 518 nm and calculated using the following equation

$$\text{antioxidant activities (\%)} = \frac{A_{\text{Blank}} - A_{\text{Film}}}{A_{\text{Blank}}} \times 100 \qquad (5)$$

where A_{Blank} was the absorbance value of DPPH and A_{Film} was the absorbance value of the DPPH containing film. The film solution was analyzed for at least five concentrations ranging from 0.25 to 4 mg mL^{-1} to obtain half-maximal inhibitory concentration (IC$_{50}$).

UV−Vis Spectrophotometry. The UV-blocking properties of the films ($2 \times 1\ \text{cm}^2$) were determined by a UV−vis spectrophotometer (V-570, Jasco Corp., Japan). The wavelength of 550 nm was used to determine the film transparency. The % transmittances at the wavelengths between 275 and 320 nm and between 320 and 380 nm were observed for UV-B and UV-A absorption, respectively.[73]

Mechanical Properties. A universal testing machine (LTS-500N-S2, Minebea Co., Ltd., Japan) equipped with a load cell of 500 N was used to determine tensile strength, elongation at break, and Young's modulus according to the ASTM D 882 standard method. The films ($10 \times 1\ \text{cm}^2$) were inserted between two jaws of the machine (5 cm gauge length) and stretched at a rate of 10 mm min^{-1}.

Statistical Analysis. All measurements were conducted in triplicate. Data were presented as average value ± 1 standard deviation. One-way analysis of variance (ANOVA) followed by Duncan's multiple range test (DMRT) to compare any significant differences among average values at the level of $p < 0.05$ were analyzed using IBM SPSS Statistics 22 (IBM Corp., Armonk, NY).

■ AUTHOR INFORMATION

Corresponding Author

    Sehanat Prasongsuk − *Plant Biomass Utilization Research Unit, Department of Botany, Faculty of Science, Chulalongkorn University, Bangkok 10330, Thailand;* *Department of Biology, Faculty of Science and Technology, Airlangga University, Surabaya 60115, Indonesia;* orcid.org/0000-0001-5617-1077; Phone: +662-218-9191; Email: sehanat.p@chula.ac.th; Fax: +662-252-8979

Authors

    Muhammad T. Haqiqi − *Program in Biotechnology, Faculty of Science, Chulalongkorn University, Bangkok 10330, Thailand; Plant Biomass Utilization Research Unit, Department of Botany, Faculty of Science, Chulalongkorn University, Bangkok 10330, Thailand*

    Wichanee Bankeeree − *Plant Biomass Utilization Research Unit, Department of Botany, Faculty of Science, Chulalongkorn University, Bangkok 10330, Thailand*

    Pongtharin Lotrakul − *Plant Biomass Utilization Research Unit, Department of Botany, Faculty of Science, Chulalongkorn University, Bangkok 10330, Thailand*

    Prasit Pattananuwat − *Department of Materials Science, Faculty of Science, Chulalongkorn University, Bangkok 10330, Thailand*

    Hunsa Punnapayak − *Plant Biomass Utilization Research Unit, Department of Botany, Faculty of Science, Chulalongkorn University, Bangkok 10330, Thailand; Department of Biology, Faculty of Science and Technology, Airlangga University, Surabaya 60115, Indonesia*

    Rico Ramadhan − *Department of Chemistry, Faculty of Science and Technology and Division of Exploration and Synthesis of Bioactive Compound, Research Center for Bio-Molecule Engineering, Airlangga University, Surabaya 60115, Indonesia*

    Takaomi Kobayashi − *Department of Materials Science and Technology, Nagaoka University of Technology, Nagaoka 940-2188, Japan*

    Rudianto Amirta − *Faculty of Forestry, Mulawarman University, Samarinda 75124, Indonesia*

Complete contact information is available at:
https://pubs.acs.org/10.1021/acsomega.1c00249

Notes
The authors declare no competing financial interest.

■ REFERENCES

(1) Sigler, M. The effects of plastic pollution on aquatic wildlife: current situations and future solutions. *Water, Air, Soil Pollut.* **2014**, *225*, No. 2184.

(2) Verma, R.; Vinoda, K.; Papireddy, M.; Gowda, A. Toxic pollutants from plastic waste-a review. *Procedia Environ. Sci.* **2016**, *35*, 701−708.

(3) Singh, N.; Hui, D.; Singh, R.; Ahuja, I.; Feo, L.; Fraternali, F. Recycling of plastic solid waste: A state of art review and future applications. *Composites, Part B* **2017**, *115*, 409−422.

(4) Wang, W.; Themelis, N. J.; Sun, K.; Bourtsalas, A. C.; Huang, Q.; Zhang, Y.; Wu, Z. Current influence of China's ban on plastic waste imports. *Waste Disposal Sustainable Energy* **2019**, *1*, 67−78.

(5) Horodytska, O.; Valdés, F. J.; Fullana, A. Plastic flexible films waste management—A state of art review. *Waste Manage.* **2018**, *77*, 413−425.

(6) Jha, P. Effect of plasticizer and antimicrobial agents on functional properties of bionanocomposite films based on corn starch-chitosan for food packaging applications. *Int. J. Biol. Macromol.* **2020**, *160*, 571−582.

(7) Benítez, A. J.; Walther, A. Cellulose nanofibril nanopapers and bioinspired nanocomposites: a review to understand the mechanical property space. *J. Mater. Chem. A* **2017**, *5*, 16003−16024.

(8) Huang, C.; Dong, H.; Zhang, Z.; Bian, H.; Yong, Q. Procuring the nano-scale lignin in prehydrolyzate as ingredient to prepare cellulose nanofibril composite film with multiple functions. *Cellulose* **2020**, *27*, 9355−9370.

(9) He, X.; Luzi, F.; Hao, X.; Yang, W.; Torre, L.; Xiao, Z.; Xie, Y.; Puglia, D. Thermal, antioxidant and swelling behaviour of transparent polyvinyl (alcohol) films in presence of hydrophobic citric acid-modified lignin nanoparticles. *Int. J. Biol. Macromol.* **2019**, *127*, 665−676.

(10) Bian, H.; Chen, L.; Dong, M.; Wang, L.; Wang, R.; Zhou, X.; Wu, C.; Wang, X.; Ji, X.; Dai, H. Natural lignocellulosic nanofibril film with excellent ultraviolet blocking performance and robust environment resistance. *Int. J. Biol. Macromol.* **2021**, *166*, 1578−1585.

(11) Wei, Z.; Cai, C.; Huang, Y.; Wang, P.; Song, J.; Deng, L.; Fu, Y. Strong biodegradable cellulose materials with improved crystallinity via hydrogen bonding tailoring strategy for UV blocking and antioxidant activity. *Int. J. Biol. Macromol.* **2020**, *164*, 27−36.

(12) Sirviö, J. A.; Ismail, M. Y.; Zhang, K.; Tejesvi, M. V.; Ämmälä, A. Transparent lignin-containing wood nanofiber films with UV-blocking, oxygen barrier, and anti-microbial properties. *J. Mater. Chem. A* **2020**, *8*, 7935−7946.

(13) Mahmoudian, S.; Wahit, M. U.; Ismail, A.; Yussuf, A. Preparation of regenerated cellulose/montmorillonite nanocomposite films via ionic liquids. *Carbohydr. Polym.* **2012**, *88*, 1251−1257.

(14) Pang, J.; Liu, X.; Zhang, X.; Wu, Y.; Sun, R. Fabrication of cellulose film with enhanced mechanical properties in ionic liquid 1-allyl-3-methylimidaxolium chloride (AmimCl). *Materials* **2013**, *6*, 1270−1284.

(15) Chua, K. Y.; Azzahari, A. D.; Abouloula, C. N.; Sonsudin, F.; Shahabudin, N.; Yahya, R. Cellulose-based polymer electrolyte derived from waste coconut husk: residual lignin as a natural plasticizer. *J. Polym. Res.* **2020**, *27*, No. 115.

(16) Rachtanapun, P.; Luangkamin, S.; Tanprasert, K.; Suriyatem, R. Carboxymethyl cellulose film from durian rind. *LWT—Food Sci. Technol.* **2012**, *48*, 52−58.

(17) Tavares, K. M.; de Campos, A.; Mitsuyuki, M. C.; Luchesi, B. R.; Marconcini, J. M. Corn and cassava starch with carboxymethyl cellulose films and its mechanical and hydrophobic properties. *Carbohydr. Polym.* **2019**, *223*, No. 115055.

(18) El-Sayed, S.; Mahmoud, K.; Fatah, A.; Hassen, A. DSC, TGA and dielectric properties of carboxymethyl cellulose/polyvinyl alcohol blends. *Phys. B: Condens. Matter* **2011**, *406*, 4068−4076.

(19) Jiang, B.; Yu, J.; Luo, X.; Zhu, Y.; Jin, Y. A strategy to improve enzymatic saccharification of wheat straw by adding water-soluble lignin prepared from alkali pretreatment spent liquor. *Process Biochem.* **2018**, *71*, 147−151.

(20) Dahnum, D.; Tasum, S. O.; Triwahyuni, E.; Nurdin, M.; Abimanyu, H. Comparison of SHF and SSF processes using enzyme and dry yeast for optimization of bioethanol production from empty fruit bunch. *Energy Procedia* **2015**, *68*, 107−116.

(21) Ahmad, F. B.; Zhang, Z.; Doherty, W. O.; O'Hara, I. M. The outlook of the production of advanced fuels and chemicals from integrated oil palm biomass biorefinery. *Renewable Sustainable Energy Rev.* **2019**, *109*, 386−411.

(22) Chang, S. H. J. B. An overview of empty fruit bunch from oil palm as feedstock for bio-oil production. *Biomass Bioenergy* **2014**, *62*, 174−181.

(23) Amin, M. C. I.; Soom, R.; Ahmad, I.; Lian, H. H. Carboxymethyl cellulose from palm oil empty fruit bunch—their

properties and use as a film coating agent. *J. Sains Kesihatan Malays.* **2007**, *4*, 53−62.

(24) Santos, R. B.; Hart, P.; Jameel, H.; Chang, H.-m. Wood based lignin reactions important to the biorefinery and pulp and paper industries. *BioResources* **2012**, *8*, 1456−1477.

(25) Li, J.; Zhang, S.; Li, H.; Ouyang, X.; Huang, L.; Ni, Y.; Chen, L. Cellulase pretreatment for enhancing cold caustic extraction-based separation of hemicelluloses and cellulose from cellulosic fibers. *Bioresour. Technol.* **2018**, *251*, 1−6.

(26) Akhtar, J.; Teo, C. L.; Lai, L. W.; Hassan, N.; Idris, A.; Aziz, R. A. Factors affecting delignification of oil palm empty fruit bunch by microwave-assisted dilute acid/alkali pretreatment. *BioResources* **2015**, *10*, 588−596.

(27) Saito, K.; Horikawa, Y.; Sugiyama, J.; Watanabe, T.; Kobayashi, Y.; Takabe, K. Effect of thermochemical pretreatment on lignin alteration and cell wall microstructural degradation in *Eucalyptus globulus*: comparison of acid, alkali, and water pretreatments. *J. Wood Sci.* **2016**, *62*, 276−284.

(28) Liu, W.; Chen, W.; Hou, Q.; Wang, S.; Liu, F. Effects of combined pretreatment of dilute acid pre-extraction and chemical-assisted mechanical refining on enzymatic hydrolysis of lignocellulosic biomass. *RSC Adv.* **2018**, *8*, 10207−10214.

(29) Huang, C.; Sun, R.; Chang, H. M.; Yong, Q.; Jameel, H.; Phillips, R. Production of dissolving grade pulp from tobacco stalk through SO2-ethanol-water fractionation, alkaline extraction, and bleaching processes. *BioResources* **2019**, *14*, 5544−5558.

(30) Parid, D. M.; Abd Rahman, N. A.; Baharuddin, A. S.; Mohammed, M. A. P.; Johari, A. M.; Razak, S. Z. A. Synthesis and characterization of carboxymethyl cellulose from oil palm empty fruit bunch stalk fibres. *BioResources* **2018**, *13*, 535−554.

(31) Shui, T.; Feng, S.; Chen, G.; Li, A.; Yuan, Z.; Shui, H.; Kuboki, T.; Xu, C. Synthesis of sodium carboxymethyl cellulose using bleached crude cellulose fractionated from cornstalk. *Biomass Bioenergy* **2017**, *105*, 51−58.

(32) Mondal, M. I. H.; Yeasmin, M. S.; Rahman, M. S. Preparation of food grade carboxymethyl cellulose from corn husk agrowaste. *Int. J. Biol. Macromol.* **2015**, *79*, 144−150.

(33) Candido, R.; Gonçalves, A. Synthesis of cellulose acetate and carboxymethylcellulose from sugarcane straw. *Carbohydr. Polym.* **2016**, *152*, 679−686.

(34) Rodsamran, P.; Sothornvit, R. Rice stubble as a new biopolymer source to produce carboxymethyl cellulose-blended films. *Carbohydr. Polym.* **2017**, *171*, 94−101.

(35) Lakshmi, D. S.; Trivedi, N.; Reddy, C. Synthesis and characterization of seaweed cellulose derived carboxymethyl cellulose. *Carbohydr. Polym.* **2017**, *157*, 1604−1610.

(36) Asl, S. A.; Mousavi, M.; Labbafi, M. Synthesis and characterization of carboxymethyl cellulose from sugarcane bagasse. *J. Food Process. Technol.* **2017**, *8*, No. 1000687.

(37) Haleem, N.; Arshad, M.; Shahid, M.; Tahir, M. A. Synthesis of carboxymethyl cellulose from waste of cotton ginning industry. *Carbohydr. Polym.* **2014**, *113*, 249−255.

(38) Jiang, Y.; Zhou, J.; Zhang, Q.; Zhao, G.; Heng, L.; Chen, D.; Liu, D. Preparation of cellulose nanocrystals from Humulus japonicus stem and the influence of high temperature pretreatment. *Carbohydr. Polym.* **2017**, *164*, 284−293.

(39) de Farias, J. G. G.; Cavalcante, R. C.; Canabarro, B. R.; Viana, H. M.; Scholz, S.; Simão, R. A. Surface lignin removal on coir fibers by plasma treatment for improved adhesion in thermoplastic starch composites. *Carbohydr. Polym.* **2017**, *165*, 429−436.

(40) Ma, Z.; Sun, Q.; Ye, J.; Yao, Q.; Zhao, C. Study on the thermal degradation behaviors and kinetics of alkali lignin for production of phenolic-rich bio-oil using TGA—FTIR and Py—GC/MS. *J. Anal. Appl. Pyrol.* **2016**, *117*, 116−124.

(41) Barros, P. J. R.; Ascheri, D. P. R.; Santos, M. L. S.; Morais, C. C.; Ascheri, J. L. R.; Signini, R.; dos Santos, D. M.; de Campos, A. J.; Devilla, I. A. Soybean hulls: Optimization of the pulping and bleaching processes and carboxymethyl cellulose synthesis. *Int. J. Biol. Macromol.* **2020**, *144*, 208−218.

(42) Singh, R. K.; Singh, A. K. Optimization of reaction conditions for preparing carboxymethyl cellulose from corn cobic agricultural waste. *Waste Biomass Valorization* **2013**, *4*, 129−137.

(43) Golbaghi, L.; Khamforoush, M.; Hatami, T. Carboxymethyl cellulose production from sugarcane bagasse with steam explosion pulping: Experimental, modeling, and optimization. *Carbohydr. Polym.* **2017**, *174*, 780−788.

(44) de Diego-Díaz, B.; Duran, A.; Álvarez-García, M. R.; Fernández-Rodríguez, J. New trends in physicochemical characterization of solid lignocellulosic waste in anaerobic digestion. *Fuel* **2019**, *245*, 240−246.

(45) Michelin, M.; Liebentritt, S.; Vicente, A. A.; Teixeira, J. A. Lignin from an integrated process consisting of liquid hot water and ethanol organosolv: Physicochemical and antioxidant properties. *Int. J. Biol. Macromol.* **2018**, *120*, 159−169.

(46) Pinheiro, F. G. C.; Soares, A. K. L.; Santaella, S. T.; de Silva, L. M. A.; Canuto, K. M.; Cáceres, C. A.; de Freitas Rosa, M.; de Andrade Feitosa, J. P.; Leitão, R. C. Optimization of the acetosolv extraction of lignin from sugarcane bagasse for phenolic resin production. *Ind. Crops Prod.* **2017**, *96*, 80−90.

(47) Tan, X.; Zhang, Q.; Wang, W.; Zhuang, X.; Deng, Y.; Yuan, Z. Comparison study of organosolv pretreatment on hybrid pennisetum for enzymatic saccharification and lignin isolation. *Fuel* **2019**, *249*, 334−340.

(48) Wu, D.; Chang, P. R.; Ma, X. Preparation and properties of layered double hydroxide−carboxymethylcellulose sodium/glycerol plasticized starch nanocomposites. *Carbohydr. Polym.* **2011**, *86*, 877−882.

(49) Wang, J.; Qian, Y.; Deng, Y.; Liu, D.; Li, H.; Qiu, X. Probing the interactions between lignin and inorganic oxides using atomic force microscopy. *Appl. Surf. Sci.* **2016**, *390*, 617−622.

(50) Shankar, S.; Rhim, J.-W. Preparation and characterization of agar/lignin/silver nanoparticles composite films with ultraviolet light barrier and antibacterial properties. *Food Hydrocolloids* **2017**, *71*, 76−84.

(51) Izaguirre, N.; Gordobil, O.; Robles, E.; Labidi, J. Enhancement of UV absorbance and mechanical properties of chitosan films by the incorporation of solvolytically fractionated lignins. *Int. J. Biol. Macromol.* **2020**, *155*, 447−455.

(52) Mirzaei-Mohkam, A.; Garavand, F.; Dehnad, D.; Keramat, J.; Nasirpour, A. Physical, mechanical, thermal and structural characteristics of nanoencapsulated vitamin E loaded carboxymethyl cellulose films. *Prog. Org. Coat.* **2020**, *138*, No. 105383.

(53) Michelin, M.; Marques, A. M.; Pastrana, L. M.; Teixeira, J. A.; Cerqueira, M. A. Carboxymethyl cellulose-based films: Effect of organosolv lignin incorporation on physicochemical and antioxidant properties. *J. Food Eng.* **2020**, No. 110107.

(54) Kiuru, M.; Alakoski, E. Low sliding angles in hydrophobic and oleophobic coatings prepared with plasma discharge method. *Mater. Lett.* **2004**, *58*, 2213−2216.

(55) Crouvisier-Urion, K.; Bodart, P. R.; Winckler, P.; Raya, J.; Gougeon, R. D.; Cayot, P.; Domenek, S.; Debeaufort, F.; Karbowiak, T. Biobased composite films from chitosan and lignin: antioxidant activity related to structure and moisture. *ACS Sustainable Chem. Eng.* **2016**, *4*, 6371−6381.

(56) Zadeh, E. M.; O'Keefe, S. F.; Kim, Y.-T. Utilization of lignin in biopolymeric packaging films. *ACS Omega* **2018**, *3*, 7388−7398.

(57) Chinma, C. E.; Ariahu, C. C.; Alakali, J. S. Effect of temperature and relative humidity on the water vapour permeability and mechanical properties of cassava starch and soy protein concentrate based edible films. *J. Food Sci. Technol.* **2015**, *52*, 2380−2386.

(58) El-Sakhawy, M.; Tohamy, H.-A. S.; Salama, A.; Kamel, S. J. C. C. Thermal properties of carboxymethyl cellulose acetate butyrate. *Cellul. Chem. Technol.* **2019**, *53*, 667−675.

(59) Suppiah, K.; Leng, T. P.; Husseinsyah, S.; Rahman, R.; Keat, Y. C.; Heng, C. Thermal properties of carboxymethyl cellulose (CMC) filled halloysite nanotube (HNT) bio-nanocomposite films. *Mater. Today: Proc.* **2019**, *16*, 1611−1616.

(60) Oun, A. A.; Rhim, J.-W. Preparation of multifunctional carboxymethyl cellulose-based films incorporated with chitin nanocrystal and grapefruit seed extract. *Int. J. Biol. Macromol.* **2020**, *152*, 1038−1046.

(61) Monteiro, S. N.; Calado, V.; Margem, F. M.; Rodriguez, R. J. Thermogravimetric stability behavior of less common lignocellulosic fibers - a review. *J. Mater. Res. Technol.* **2012**, *1*, 189−199.

(62) Roman, M.; Winter, W. T. Effect of sulfate groups from sulfuric acid hydrolysis on the thermal degradation behavior of bacterial cellulose. *Biomacromolecules* **2004**, *5*, 1671−1677.

(63) Avelino, F.; de Oliveira, D. R.; Mazzetto, S. E.; Lomonaco, D. Poly(methyl methacrylate) films reinforced with coconut shell lignin fractions to enhance their UV-blocking, antioxidant and thermo-mechanical properties. *Int. J. Biol. Macromol.* **2019**, *125*, 171−180.

(64) Dong, H.; Zheng, L.; Yu, P.; Jiang, Q.; Wu, Y.; Huang, C.; Yin, B. Characterization and application of lignin−carbohydrate complexes from lignocellulosic materials as antioxidants for scavenging in vitro and in vivo reactive oxygen species. *ACS Sustainable Chem. Eng.* **2020**, *8*, 256−266.

(65) Tian, D.; Hu, J.; Bao, J.; Chandra, R. P.; Saddler, J. N.; Lu, C. Lignin valorization: Lignin nanoparticles as high-value bio-additive for multifunctional nanocomposites. *Biotechnol. Biofuels* **2017**, *10*, No. 1.

(66) Aadil, K. R.; Barapatre, A.; Jha, H. Synthesis and characterization of Acacia lignin-gelatin film for its possible application in food packaging. *Bioresour. Bioprocess.* **2016**, *3*, No. 27.

(67) Ugartondo, V.; Mitjans, M.; Vinardell, M. P. Comparative antioxidant and cytotoxic effects of lignins from different sources. *Bioresour. Technol.* **2008**, *99*, 6683−6687.

(68) Pei, W.; Chen, Z. S.; Chan, H. Y. E.; Zheng, L.; Liang, C.; Huang, C. Isolation and identification of a novel anti-protein aggregation activity of lignin-carbohydrate complex from *Chionanthus retusus* leaves. *Front. Bioeng. Biotechnol* **2020**, *8*, No. 573991.

(69) Guo, Y.; Tian, D.; Shen, F.; Yang, G.; Long, L.; He, J.; Song, C.; Zhang, J.; Zhu, Y.; Huang, C.; Deng, S. Transparent cellulose/ technical lignin composite films for advanced packaging. *Polymers* **2019**, *11*, No. 1455.

(70) Sadeghifar, H.; Venditti, R.; Jur, J.; Gorga, R. E.; Pawlak, J. J. Cellulose-lignin biodegradable and flexible UV protection film. *ACS Sustainable Chem. Eng.* **2017**, *5*, 625−631.

(71) Posoknistakul, P.; Tangkrakul, C.; Chaosuanphae, P.; Deepentham, S.; Techasawong, W.; Phonphirunrot, N.; Bairak, S.; Sakdaronnarong, C.; Laosiripojana, N. Fabrication and characterization of lignin particles and their ultraviolet protection ability in PVA composite film. *ACS Omega* **2020**, *5*, 20976−20982.

(72) Parit, M.; Saha, P.; Davis, V. A.; Jiang, Z. Transparent and homogenous cellulose nanocrystal/lignin UV-protection films. *ACS Omega* **2018**, *3*, 10679−10691.

(73) Zhang, X.; Liu, W.; Liu, W.; Qiu, X. High performance PVA/ lignin nanocomposite films with excellent water vapor barrier and UV-shielding properties. *Int. J. Biol. Macromol.* **2020**, *142*, 551−558.

(74) Yang, W.; Owczarek, J.; Fortunati, E.; Kozanecki, M.; Mazzaglia, A.; Balestra, G.; Kenny, J.; Torre, L.; Puglia, D. Antioxidant and antibacterial lignin nanoparticles in polyvinyl alcohol/chitosan films for active packaging. *Ind. Crops Prod.* **2016**, *94*, 800−811.

(75) Yadav, M.; Behera, K.; Chang, Y.-H.; Chiu, F.-C. Cellulose Nanocrystal Reinforced Chitosan Based UV Barrier Composite Films for Sustainable Packaging. *Polymers* **2020**, *12*, No. 202.

(76) Kargarzadeh, H.; Galeski, A.; Pawlak, A. PBAT green composites: Effects of kraft lignin particles on the morphological, thermal, crystalline, macro and micromechanical properties. *Polymer* **2020**, No. 122748.

(77) Lim, C. W. Is a nanorod (or nanotube) with a lower Young's modulus stiffer? Is not Young's modulus a stiffness indicator? *Sci. China: Phys., Mech. Astron.* **2010**, *53*, 712−724.

(78) Vena, P.; García-Aparicio, M.; Brienzo, M.; Görgens, J.; Rypstra, T. Impact of hemicelluloses pre-extraction of pulp properties of sugarcane bagasse. *Cellul. Chem. Technol.* **2013**, *47*, 425−441.

(79) Tristantini, D.; Yunan, A. Advanced characterization of microbeads replacement from cellulose acetate based on empty fruit bunches and dried jackfruit leaves. *E3S Web Conf.* **2018**, No. 04045.

(80) Goering, I. K.; Van Soest, P. J. *Forage Fiber Analysis (Apparatus, Reagents, Procedures and Some Application)*; U.S. Government Publishing Office: Washington, 1970.

(81) Jouki, M.; Khazaei, N.; Ghasemlou, M.; HadiNezhad, M. Effect of glycerol concentration on edible film production from cress seed carbohydrate gum. *Carbohydr. Polym.* **2013**, *96*, 39–46.

(82) Cazón, P.; Velázquez, G.; Vázquez, M. Characterization of bacterial cellulose films combined with chitosan and polyvinyl alcohol: Evaluation of mechanical and barrier properties. *Carbohydr. Polym.* **2019**, *216*, 72–85.

(83) Shankar, S.; Wang, L.-F.; Rhim, J.-W. Effect of melanin nanoparticles on the mechanical, water vapor barrier, and antioxidant properties of gelatin-based films for food packaging application. *Food Packag. Shelf Life* **2019**, *21*, No. 100363.